Int J Earth Sci (Geol Rundsch) (2016) 105:1549–1562
DOI 10.1007/s00531-015-1268-x

ORIGINAL PAPER

Analysis of 6-year fluid electric conductivity logs to evaluate the hydraulic structure of the deep drill hole at Outokumpu, Finland

Prabhakar Sharma[1,2] · Chin-Fu Tsang[2,3] · Ilmo T. Kukkonen[4] · Auli Niemi[2]

Received: 5 December 2014 / Accepted: 21 October 2015 / Published online: 6 November 2015

Abstract Over the last two decades, the flowing fluid electric conductivity (FFEC) logging method has been applied in boreholes in the well-testing mode to evaluate the transmissivity, hydraulic head, and formation water electrical conductivity as a function of depth with a resolution of about 10–20 cm. FFEC profiles along the borehole are obtained under both shut-in and pumping conditions in a logging procedure that lasts only 3 or 4 days. A method for analyzing these FFEC logs has been developed and successfully employed to obtain formation parameters in a number of field studies. The present paper concerns the analysis of a unique set of FFEC logs that were taken from a deep borehole reaching down to 2.5 km at Outokumpu, Finland, over a 6-year time period. The borehole intersects paleoproterozoic metasedimentary, granitoid, and ophiolite-derived rocks. After the well was drilled, completed, and cleaned up, FFEC logs were obtained after 7, 433, 597, 948, and 2036 days. In analyzing these five profiles, we discovered the need to account for salinity diffusion from water in the formation to the borehole. Analysis results include the identification of 15 hydraulically conducting zones along the borehole, the calculation of flow rates associated with these 15 zones, as well as the estimation of the variation of formation water electrical conductivity as a function of depth. The calculated flow rates were used to obtain the tentative hydraulic conductivity values at these 15 depth levels.

Keywords Flowing fluid electric conductivity logging · Long-term monitoring · Deep formation water electrical conductivity · Salinity diffusion · Outokumpu deep drill hole

✉ Prabhakar Sharma
psharma@nalandauniv.com

[1] School of Ecology and Environment Studies, Nalanda University, Rajgir, Nalanda, Bihar 803116, India

[2] Department of Earth Sciences, Uppsala University, Uppsala, Sweden

[3] Earth Sciences Division, Lawrence Berkeley National Laboratory, Berkeley, CA, USA

[4] Department of Physics, University of Helsinki, Helsinki, Finland

Introduction

Detailed information about the permeability structure and locations of hydraulically conductive zones and salinity variation in deep geologic layers is critical for understanding subsurface flow and transport behavior of groundwater and solutes at depth (such as petroleum products, toxic chemicals, carbon dioxide, radioactive wastes, and hydrothermal fluids). Usually, these hydraulic data are obtained through established geophysical and hydrological methods applied to deep boreholes, such as straddle-packer tests (Walton 1970), gamma and neutron logging (Keys 1986; Mendoza et al. 2010), borehole image logging (Zemanek et al. 1970; Paillet 1991), high-resolution flow logging (Molz et al. 1989; Paillet 1998), Posiva flow logging (Öhberg and Rouhiainen 2000; Ludvigson et al. 2002; Frampton and Cvetkovic 2010; Follin et al. 2014), and flowing fluid electrical conductivity (FFEC) logging (Tsang et al. 1990; Doughty and Tsang 2005; Doughty et al. 2005, 2013; Sharma et al. 2015). Among these alternative well-test methods, FFEC logging has proved to be a very effective method for uncased as well as cased (perforated) boreholes without the need of specialized instruments. An analysis procedure has also been developed to

analyze these FFEC logs to obtain detailed hydraulic information as a function of depth in the borehole with a depth resolution of about the borehole diameter.

Up to now, the FFEC method has been applied in a well-testing mode lasting a period of a few days, mainly under pumping conditions. However, it has not been used in a monitoring mode over a period of several years for natural inflow and outflow of wellbore water, under essentially no pumping condition. The focus of the present paper is to apply the FFEC analysis method to a unique data set of EC logs obtained over 6 years from a research borehole of 2.5-km depth at the Outokumpu site in Finland. In the analysis, we discovered that the long times between the logs and the very small natural flow rates required an elaboration of the FFEC method to include the coupling of borehole inflow/outflow with salinity diffusion from the formation water in the model.

Below we first provide a description of the Outokumpu site and of the FFEC logs obtained. Then the general approach for the FFEC logging and analysis method is presented, together with a discussion of the main borehole processes involved when using the FFEC method in a well-testing mode and in a long-term monitoring mode. We then apply the analysis to the 6-year EC logging data sets from which we are able to calculate flow rates in and out of the borehole with the corresponding hydraulic conductivity as a function of depth, and to estimate the formation water electrical conductivity-depth profile. Finally, a few general remarks are made on the applicability of the FFEC method to long-term monitoring of hydrogeological conditions in deep wells.

Site information and previous hydrogeological studies

In 2004–2005, a 2516-m-deep research borehole was drilled as part of Outokumpu Deep Drilling Project of the Geological Survey of Finland in eastern part of Finland. The borehole was primarily drilled for (a) revealing the geological nature of strong seismic reflectors in the upper crust in a significant ore province with Cu–Co–Zn sulfide deposits (Kukkonen 2011; Kukkonen et al. 2012), (b) geothermal studies (Kukkonen et al. 2011), (c) deep hydrogeology, fluid, and gas geochemistry (Ahonen et al. 2011; Kietäväinen et al. 2013), and (d) deep biosphere studies (Itävaara et al. 2011a, b; Nyyssönen et al. 2013). In the deep borehole, a sequence of paleoproterozoic metasedimentary, granitoid, and ophiolite-derived rocks was encountered. Although the upper 1400 m of the Outokumpu borehole was reported to be uniform mineralogically and petrophysically, the ultrasonic logs and analysis of core samples indicated microfractures in those layers (Kern et al. 2009; Schijns et al. 2012). In addition, a detailed study of the origin and composition of saline fluids and gases in the deep biosphere were carried out to understand the hydrogeochemical properties of the deep formations around the borehole (Ahonen et al. 2011; Kukkonen et al. 2011; Kietäväinen et al. 2013).

Drill stem tests were conducted during drilling breaks at about 500-m intervals which included measurement of flow and pressure build-up in a depth interval between the borehole bottom at the time and a mechanically expandable packer set at about 50 m above it. More specifically, the test was done for the intervals 480–550 and 957–997 m (Ahonen et al. 2011) and values of hydraulic conductivity were determined as 7.5×10^{-6} m/s (0.45 mm/min) and 5.3×10^{-7} m/s (0.032 mm/min), respectively. At deeper levels (1458–1507, 2007–2072, and 2465–2516 m), the test was not able to show any measurable conductivity. Although the test sections are short and do not represent the complete drilled section, the results suggest a strongly decreasing hydraulic conductivity with depth (Ahonen et al. 2011).

After the drilling process, the drilling fluid in the deep borehole was exchanged with fresh municipal tap water. Then the change in electrical conductivity (EC) along the length of the deep borehole was measured with a mud parameter probe (temperature and fluid resistivity). The changes in fluid electrical conductivity along the borehole (EC logging profile) were monitored several times from 2005 until 2011, as shown in Fig. 1. First, a profile was obtained 7 days after the drilling process, showing the initial low salinity corresponding to that of fresh water. Then, four more profiles were obtained after 433, 597, 948, and 2036 days. We call these EC logging profiles P1, P2, P3, P4, and P5, respectively. Figure 1 also shows the measured temperature-depth profile (Ahonen et al. 2011), which was essentially linear and has remained the same since 2006. The EC logging profiles are the focus of our present study.

The logging profiles P1–P4 represent practically undisturbed conditions with no significant pumping of fluid from the deeper part of the borehole. Only P5 is affected by pumping that took place between taking of P4 and P5 profiles, but the data were corrected for such pumping before using it in the FFEC analysis (see below). Fluid samplings were done five times with a tube method (Nurmi and Kukkonen 1986) in the open borehole in 2007–2011, and the total amount of fluid taken was <600 L (the total borehole volume is about 95,600 L). However, much bigger fluid volumes were pumped on several occasions during 2009–2011 (between the times of P4 and P5 logging profiles) from packer-isolated sections, and where packers could not be installed, from the open borehole at depths of major fracture zones. The volume of fluid pumped is shown in Table 1. In 2011,

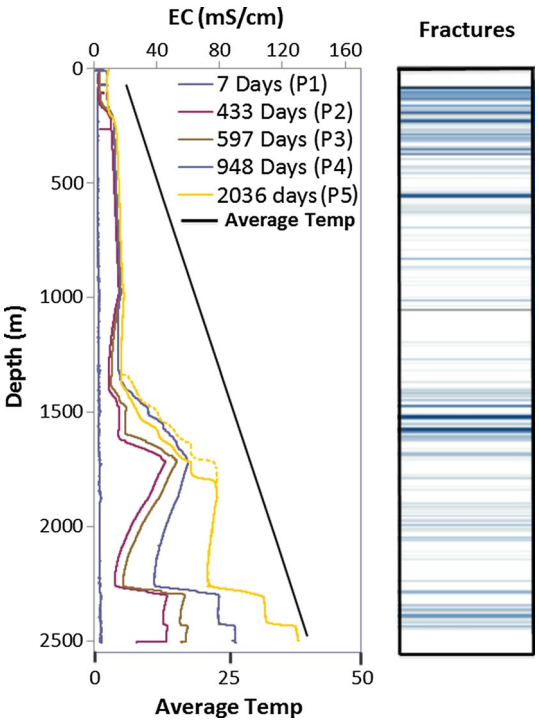

Fig. 1 Long-term logging profile (from February 2005 to September 2011) for fluid electrical conductivity measurement (*broken yellow line* shows the adjusted peak at 1715 m depth) and the borehole temperature profile from 2006 to 2008 are shown on *left*. The interpreted fracture depths using sonic, galvanic, and caliper logs are shown on *right*. The data are from the Outokumpu site (adapted from Kukkonen et al. 2011)

significant pumping was conducted at several depths, and the total volume of fluid pumped is about 29,000 L. However, pumping fluid from packer-isolated sections does not essentially alter the fluid column in the borehole, but pumping in the open borehole does. The volume of fluid pumped from the open borehole in June–August 2011 was about 8400 L. As the log P5 was conducted on September 1 only 14 days after the end of pumping, we can expect that the fluid column was disturbed by pumping. In the FFEC analysis below, we include this effect in our consideration.

The order of magnitude of flow rates into and out of the borehole was estimated with gross flow calculations and lack of characteristic flow anomalies in temperature logs by Kukkonen et al. (2011) and was found to be smaller than 0.04–0.4 mL/s, but the depths of the in- and out-flow locations could not be determined accurately. However, the in- and out-flow point locations could be determined from the FFEC logs obtained in 2005–2008: The major inflow points are at 967, 1400, 1700, 2300, and 2430 m, and major outflow points are at 220, 1300, and 2230 m.

The EC logging profiles at shallow depths (<1000 m) display steady changes over the 6-year period, in spite of various measurements and tube samplings that were made in the borehole over this time period. One possible reason is that the small aspect ratio of the flow geometry (borehole diameter being several orders of magnitude smaller than its length) limits the turbulent flow in the borehole. The borehole diameter (220 mm) is also bigger than the diameters of typical logging tools (smaller than 60 mm) and sampling tubes (10–12 mm), and thus, mechanical mixing of fluid during borehole operations is minimized.

Another reason may be that there is one or more shallow hydraulic conductive flow zones (e.g., 480–550 and 957–997 m depth interval), which have hydraulic conductivity one or two orders of magnitude larger than flow zones in the deep region (Ahonen et al. 2011), so that they shelter the deep flow zones from hydraulic disturbances in the shallow part of the well due to other measurement activities. For the purpose of analysis made in the present study with focus on the deeper section of the well, we use the assumption of zero net pumping above these deep flow zones.

The higher density fluids tend to naturally settle in the lower part of the hole, and this gravity-driven process further tends to stabilize the fluid column. On the other hand, the large borehole diameter allows local free thermal convection in the borehole, which was experimentally

Table 1 Outokumpu deep drill hole: Pumping times and rates

Year	Begin	End	Total time (days)	Depth (m)	Depth of packer 1 (m)	Depth of packer 2 (m)	Av. flow rate (L/h)	Total volume (L)	Notes
2009	11-Aug	15-Sep	35	967	960	972	6.9	5796	6
2010	27-May	20-Sep	116	2260	1189	No packer	1.7	4730	1
2010	21-Sep	11-Nov	49	500	478	502	8.6	10,100	
2011	08-Jun	02-Aug	55	2320	No packer	No packer	5.5	7260	2
2011	02-Aug	18-Aug	16	1820	No packer	No packer	3	1150	2, 3
2011	09-Sep	06-Oct	27	967	No packer	No packer	4	2600	4, 5

Notes: 1, only one packer was used; 2, no packers, pumping from open borehole; 3, flow rates varied from 2 to 7.6 L/h; 4, flow rates varied from 3.5 to 8 L/h due to gas; 5, log P5 was obtained on September 01, 2011; 6, log P4 was obtained on September 08, 2008

documented with a high-resolution stationary temperature probe in 2005 (Kukkonen et al. 2011). However, the convection cells are of about the same size vertically as the borehole diameter, which is accepted as the resolution of analysis in this paper. Thus, this effect is not directly addressed in this paper.

The fluids in the Outokumpu borehole are Na–Ca–Cl and Ca–Na–Cl-rich, and the fluids have most likely evolved from recharged meteoric water with hydrolysis of silicates under a long-term water–rock interaction (Kietäväinen et al. 2013). The stable isotopic composition suggests that the original recharge took place under a much warmer climate, i.e., tens of millions years ago. The fluid chemistry and isotope data suggest five different water types in the borehole, each originating in different fracture systems and affected by the surrounding rock types. The water types correlate with the microbial systems in the borehole, indicating very long residence times and isolation from each other and from the land surface for tens of millions of years (Kietäväinen et al. 2013). Noble gas studies support this conclusion and yield residence times of 20–50 Ma (Kietäväinen et al. 2014).

FFEC logging method

This section gives a brief summary of the general data collection and analysis methods involved in the FFEC logging. Further details of the data collection method are found in Tsang et al. (1990) and Doughty et al. (2005), and of the analysis in Doughty and Tsang (2005).

In the FFEC logging method, the wellbore water is first replaced by water of a constant salinity significantly different from that of the formation water. This may be accomplished by injecting water with low salinity, such as municipal tap water or de-ionized water, through a tube to the bottom of the wellbore at a constant rate, while simultaneously pumping from the top of the well at the same rate (water replacement phase). The goal is to replace the wellbore water with the injected water without a large change in wellbore hydraulic head, so that neither the injected water is pushed out into the formation nor the formation water is drawn into the well. The fluid electrical conductivity (EC) of the effluent is monitored at the wellhead throughout the borehole water replacement period, which continues until a low, stable EC value is reached (typically half a day or overnight for a deep 1-km well).

If the final stable effluent EC is substantially different from the EC of the injected replacement water, it indicates that the native fluid has entered the wellbore during the water replacement phase. This may occur because wellbore hydraulic head could have unintentionally dropped during recirculation or if natural regional groundwater flow is intercepted by the well. It can also occur if different

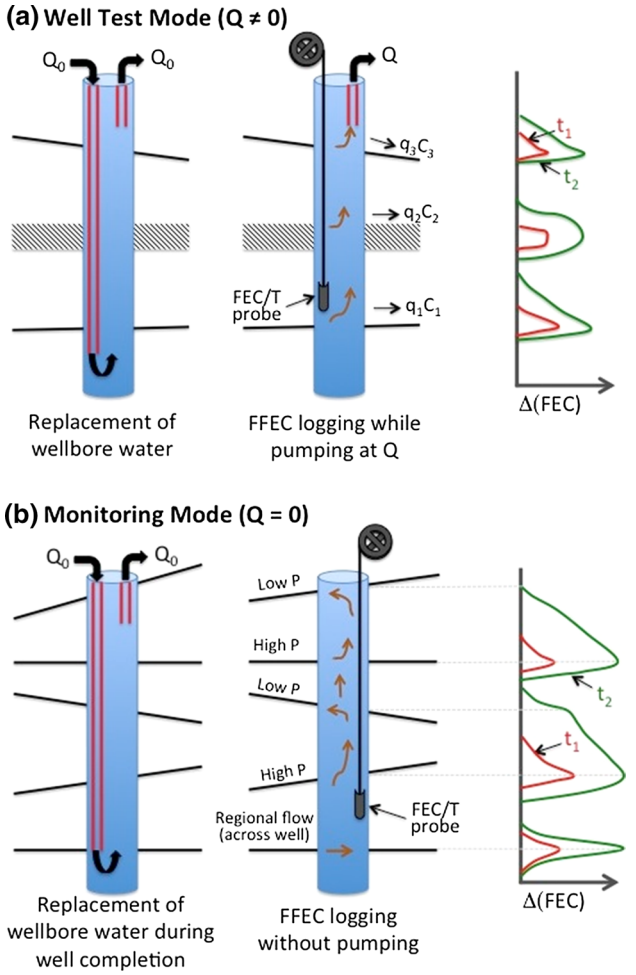

Fig. 2 Schematic diagram of FFEC logging procedure of two methods: **a** well-testing mode for pumping during logging, **b** monitoring mode for no pumping during logging operation

permeable features intercepted by the wellbore have different hydraulic heads, which sets up an internal wellbore flow, with formation water entering the wellbore through the features with higher hydraulic head and borehole water exiting to the formation through features with lower hydraulic head. Nevertheless, the method is robust and can still work as long as a carefully measured EC versus depth profile is measured after the water replacement phase and before the start of FFEC logging.

So far, the FFEC logging method has been used in a well-testing mode, in which typically the well is pumped at a constant rate, while the EC profiles are measured along the wellbore at a series of times (Fig. 2a) (Tsang et al. 1990; Doughty et al. 2005). This is accomplished by moving an electric conductivity/temperature probe up and down the wellbore, while pumping at a constant rate near the well top just below the drawdown level of the water table. The EC profiles thus obtained will display peaks in EC values

at depths where water enters into the well because of the pumping. Positions of the peaks indicate the depths of hydraulically conducting fractures or flow zones, and the size of the peaks at any time corresponds to the product of the EC of the incoming water from the flow zone, its flow rate, and the time lapse from the start of pumping. Furthermore, the EC peaks are skewed in the direction of water flow at the peak locations in the borehole. The degree of skewness is dependent on the local vertical flow rate in the borehole. These data can then be analyzed (Doughty and Tsang 2005) to obtain the inflow rate at each flow zone intercepted by the well and the EC of formation water at this depth. Furthermore, if the procedure is repeated using one or two more pumping rates at the top of the well, analysis of the data would also yield the initial hydraulic heads of the flow zones at different depths, which could be different from each other (Tsang and Doughty 2003).

The above procedure is typically used for FFEC logging in the well-testing mode lasting a few days to a week. The present paper, however, is concerned with FFEC logging in the monitoring mode, with data obtained over a period of years. In the monitoring mode, the well is usually not pumped (or if pumping has occurred over this time, its rate and duration should be recorded and subsequently accounted for in data analysis). Under such a condition, the EC profile will be dominated by "regional" flow across the well and internal flow within the borehole caused by pressure head differences between flow zones at different depths. Inflows from zones of higher heads can be identified by peaks and their spread in the borehole over time. Outflows into zones of lower heads can be detected by abrupt changes in slope of the EC profiles (Fig. 2b). These can be evaluated by the usual curve fitting techniques. In addition, slower processes will become important in the monitoring phase. In this paper, we identify the need to account for salinity diffusion between the formation water and borehole water. Furthermore, over the long monitoring period, flow rates at some of the flow zones may change due to regional effects. Such changes can also be estimated in data analysis of FFEC logging in the monitoring mode assuming that an adequate number of logging profiles have been measured.

Below we shall present the analysis of the set of FFEC logging data obtained from the deep borehole at Outokumpu over 6 years in the monitoring mode.

Analysis of FFEC logging data

EC versus depth profiles

For the monitoring mode, the FFEC logging data can be evaluated to understand the cross flow between different conductive layers penetrated by the well and their changes. Calculations of EC profiles are made (forward calculation) in which the sum of the inflows into the well is set to be equal to the sum of the outflows from the wellbore and assuming that there is no internal circulation within the borehole due to its small aspect ratio (ratio of borehole diameter to its length). In this process, the salinity of the formation water entering the wellbore will mix with that of the borehole water at a mixing strength controlled by a dispersion parameter D_{well} within the well causing a change in the fluid electrical conductivity. The EC profiles will display peaks with spread-out shoulders at depth locations where the formation water enters the wellbore at different rates as shown schematically in Fig. 2b. In the case of significant pumping of fluid from the borehole occurred over the time period, the volume produced can be taken into account through an outflow point near the top of the borehole.

For water of the same salinity, its EC value depends on its temperature. We use a correction given by Tsang et al. (1990) to convert EC values to those equivalent of water at 20 °C

$$\text{EC} = \frac{\text{EC at } T}{1 + S(T - 20)} \tag{1}$$

where $S = 0.024\ ^{\circ}\text{C}^{-1}$. In what follows, this correction has been applied and all data of EC presented are equivalent values at 20 °C.

The salinity of water in g/L is related to the measured electric conductivity (EC) linearly over the range of values of interest in our study (Snoeyink and Jenkins 1980) and we use the conversion provided by Tsang et al. (1990):

$$\text{EC} = 1870\ \text{C} \tag{2}$$

where C is salinity of formation fluid (in g/L) at 20 °C and EC is fluid electric conductivity (in mS/cm). Because of this linear relationship, C and EC can be used interchangeably with this conversion factor in mind between the two respective units.

In order to obtain the position of inflow points, the water flow rates, and EC of the formation water, we fit these EC profiles to the one-dimensional advection–dispersion numerical model. We accomplish this by using the BORE-II code developed by Doughty and Tsang (2005), using a trial and error method. The inflow locations can be identified simply by examining the early time EC profiles; however, the outflow locations, the inflow EC, and the flow rates are estimated through the application of the BORE-II code.

Study of Outokumpu EC data

At the Outokumpu deep borehole, the electrical conductivity of borehole water was monitored from a depth of 8–2516 m to estimate the salinity of the formation water, as

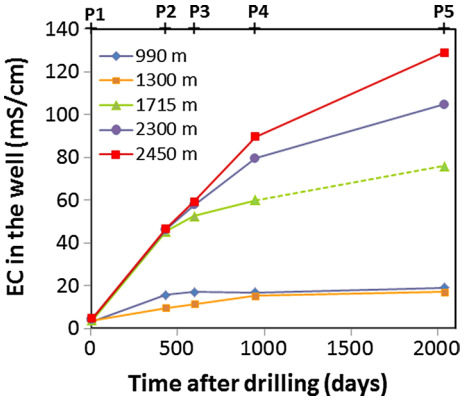

Fig. 3 Time-dependent changes in peak electrical conductivity (salinity) values of wellbore water at different depths. The *dotted line* shows the adjusted peak EC value at 1715 m depth

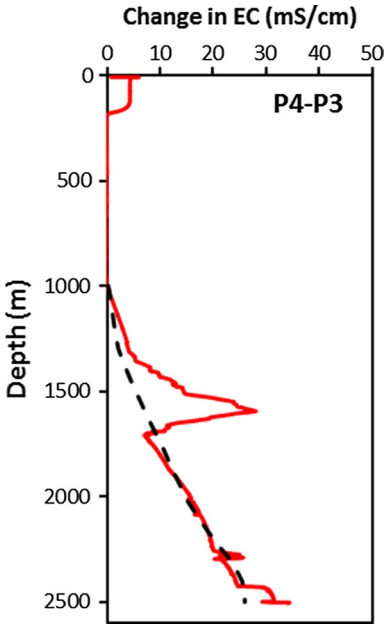

Fig. 4 Change in EC between two profiles and their baseline. The *solid line denotes* the change in profiles (P4 and P3) and *dotted line indicates* the baseline representing the result of salt diffusion from formation water into the well

shown in Fig. 1. After a qualitative study of the five sets of data P1–P5 obtained over the 6 years, we observed that EC in the borehole down to about 1000 m depth has reached a saturation value within 1 year, but EC of the borehole water deeper in the borehole was still increasing up to the last measurement performed in 2011 (Fig. 3). We also noticed a small downward shift in the pronounced peak (as indicated by dotted line in Fig. 1) at the depth of 1715 m over a period of approximately 3 years between the P4 and P5 profiles. We attribute this due to the extensive pumping of fluid (approximately 8400 L) from the borehole from 2320 to 1820 m depth levels in the preceding 2–3 months (Table 1) as discussed in "Site information and previous hydrogeological." To account for this discrepancy between logs P4 and P5, we decided to shift this particular peak of the P5 profile upward so that the peak remains at the same depth as in the previous profiles (as it should be), and conduct the analysis with this modified P5 profile. We believe the results will not be much affected by this procedure due to the robustness of the method.

The constant salinity of borehole water at the upper part of the well indicates that EC of the formation water could be in the range of 20 mS/cm, consistent with available measurements of salinity logging profiles for the top 1400-m section of the borehole. From a depth of 1400 m to the peak at 1715 m, the EC profiles P4 and P5 approximately overlap each other (see Fig. 1), meaning no more increase in salinity/EC over the time periods in between. Further, the profiles follow a linear trend in this interval. On the other hand, EC of borehole water deeper than 1715 m appears to be still increasing even when the last measurement was made (P5 profile in Fig. 1, see also Fig. 3). All this information guides us to assume that the formation water EC as a function of depth follows a trend: constant EC down to 1400 m, then linear trend given by the mean of P4 and P5 EC profiles between 1400 and 1715 m, and finally a linearly increasing profiles from 1715 m down to a value of $EC_{R,max}$ at the bottom of the borehole at 2500 m depth, where $EC_{R,max}$ is to be determined by fitting the EC profiles. This EC depth profile, with one fitting parameter $EC_{R,max}$, is the simplest possible profile to describe the depth dependence of the formation water EC. Additional features to this EC depth profile can be added if needed to match the profiles P2–P5.

Study of FEC differences between FFEC logs

In order to understand the rate of increase in EC as a function of depth in the borehole at different times, the difference between measured EC profiles (P4 and P3) was obtained as shown in Fig. 4. The difference between profiles P4 and P3 indicates EC peaks or inflows at approximately 1600, 2275, and 2430 m depth. In addition to these peaks, which result from inflows of formation water into the well through hydraulically conductive fractures at these particular depths, a linear increase in "background" EC with depth was observed (below 1400 m depth), as indicated in Fig. 4. After exploring several possible alternative reasons for this behavior, this "smooth" increase in EC with depth is interpreted as the result of salinity diffusion from the surrounding formation water to the borehole water in the uncased well due to their high difference in salinity and the long time periods between the profiles. To study this effect, we proceed as discussed in the next subsection.

Salinity diffusion between the wellbore water and neighboring formation

To account for salinity diffusion from the rock into the borehole water is not straight forward because water salinity in the borehole is changing with time owing to inflows and outflows through hydraulically conductive layers or fractures intercepted by the borehole. However, we have measured data of EC profile over time in the borehole, which is directly proportional to salinity according to Eq. (2). Since the focus of the present study is not on the salinity diffusion but on the estimation of hydraulic properties of inflow/outflow zones, we chose an approximate approach by assuming that the mass diffusion rate into the borehole is at steady state at any time, which may be justifiable on the long time frame of years covered by the data. In this case, the diffusion of formation water salinity into the wellbore can be represented by Fick's first law of diffusion as:

$$J = D \cdot 2\pi H \cdot \frac{\Delta C}{\ln\left(R_{\text{large}}/r_w\right)} \tag{3}$$

where J is mass salinity flux, D is solute diffusion coefficient in the rock, H is vertical section length of the wellbore in our calculation, r_w is wellbore radius, and R_{large} is a value of radial distance where the formation water salinity can be assumed to remain constant with time. Further, $\Delta C = (C_R - C_{av})$ is salinity difference, C_R is formation water salinity, and C_{av} is average salinity in wellbore over the time period of two adjacent profiles. For the present analysis, we assume the length of the borehole to be discretized into 50-m intervals; thus $H = 50$ m. Equation (3) may be rewritten as:

$$J = \alpha\ \Delta C \tag{3a}$$

by setting $\alpha = \frac{D \cdot 2\pi H}{\ln(R_{\text{large}}/r_w)}$. Note that because of the logarithm, the dependence of α on R_{large}/r_w is relatively small. We assume that α is a constant for the present study.

In order to calculate the formation water salinity C_R, the mass flux across the wellbore is first calculated as a function of well depth by summing over all the 50 m depth intervals as follows:

$$\sum J(P_5 - P_4) = \sum M(P_5 - P_4)/T(P_{45}) = \alpha\left(\sum C_{R1} - \sum C_{av}(P_{45})\right) \tag{4}$$

and

$$\sum J(P_4 - P_3) = \sum M(P_4 - P_3)/T(P_{34}) = \alpha\left(\sum C_{R1} - \sum C_{av}(P_{34})\right) \tag{5}$$

where $\Sigma J\ (P_5 - P_4)$ and $\Sigma J\ (P_4 - P_3)$ are the summation of mass flux over the entire depth of the well, for the time intervals represented by the P5–P4 and P4–P3, respectively. $\Sigma M\ (P_5 - P_4)$ and $\Sigma M\ (P_4 - P_3)$ are the total mass entered into the well for profile P5–P4 and profile P4–P3, respectively, $T\ (P_{45})$ and $T\ (P_{34})$ are the time interval for profile P5–P4 and P4–P3, respectively, ΣC_{R1} is the sum of formation water salinity over all the 50-m intervals to be estimated using the combination of P5–P4 and P4–P3 profiles, and $\Sigma C_{\text{av}}\ (P_{45})$ and $\Sigma C_{\text{av}}\ (P_{34})$ are sum of the average salinity in wellbore over the time intervals for profile P5–P4 and P4–P3, respectively. In order to solve Eqs. (4) and (5) for ΣC_{R1}, we divide the two equations to cancel the α factor and obtain:

$$\frac{\sum M(P_5 - P_4)}{\sum M(P_4 - P_3)} = \beta_1 = \frac{\left(\sum C_{R1} - \sum C_{av}(P_{45})\right)T_{45}}{\left(\sum C_{R1} - \sum C_{av}(P_{34})\right)T_{34}} \tag{6}$$

where β_1 is the ratio of the total salt mass entered into the wellbore over the time periods between profiles P5 and P4 and then P4 and P3, respectively. After solving Eq. (6), the total formation water salinity is obtained by:

$$\sum C_{R1} = \frac{\sum C_{av}(P_{45}) \cdot T_{45} - \beta_1 \sum C_{av}(P_{34}) \cdot T_{34}}{T_{45} - T_{34}\beta_1} \tag{7}$$

Similarly, we also used the combination of profile P4–P3 and P3–P2 to obtain another set of total formation water salinity as:

$$\sum C_{R2} = \frac{\sum C_{av}(P_{34}) \cdot T_{34} - \beta_2 \sum C_{av}(P_{23}) \cdot T_{23}}{T_{34} - T_{23}\beta_2} \tag{8}$$

where ΣC_{R2} is the sum of total formation water salinity estimated using the combination of P4–P3 and P3–P2 profiles and β_2 is the ratio of the total salt mass entered into the wellbore over time periods of P4 and P3 and then P3 and P2, respectively. Given the results of ΣC_{R1} and ΣC_{R2} from Eqs. (7) and (8), we can use the EC depth profiles as described at the end of "Study of Outokumpu EC data" section (with their conversion to salinity through Eq. 2) to calculate the maximum C_R values at 2500 m, i.e., $C_{R1,\max}$ and $C_{R2,\max}$. Ideally, the results from Eqs. (7) and (8) should be the same, i.e., $C_{R1,\max} = C_{R2,\max}$, and the difference indicates accuracy of field data.

Calculation of $C_{R1,\max}$ or $EC_{R1,\max}$ from field data

To apply the equations on salinity in the last subsection to field data which are measurements of EC, we just need to recognize the linear relationship between salinity and EC as given by Eq. (2), so that all the equations are applicable directly to EC data so long as EC is used consistently to replace salinity. With this in mind, EC data are inputted into Eqs. (7) and (8) and the results are shown in Fig. 5, which shows the dependence of $C_{R1,\max}$ and $C_{R2,\max}$ on β_1 and β_2, respectively, using the simple average of EC data at the appropriate times, with and without the time weighting.

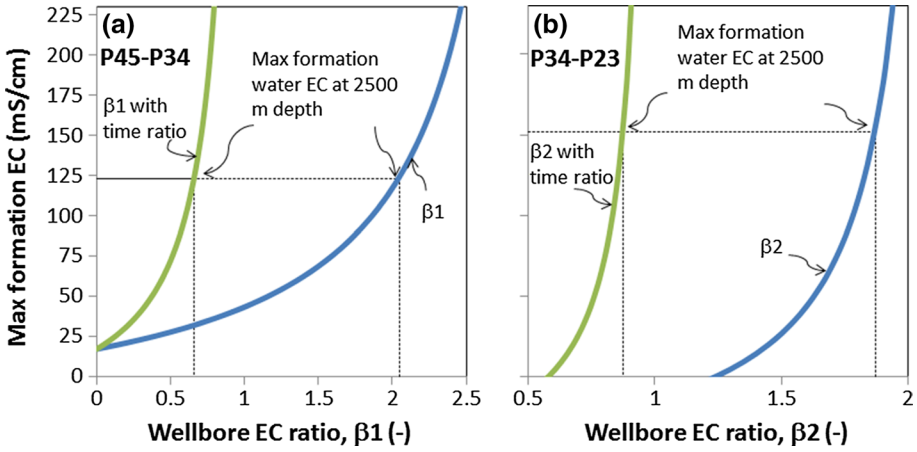

Fig. 5 Relationship between the ratio of salt mass (EC equivalent) change β_1 and β_2 and the maximum formation water EC ($EC_{R1,max}$ and $EC_{R2,max}$) at 2500 m depth using **a** P45–P34 and **b** P34–P23 profiles. β_1 with time ratio is equal to $\beta_1 T_{34}/T_{45}$ and β_2 with time ratio is equal to $\beta_2 T_{23}/T_{34}$

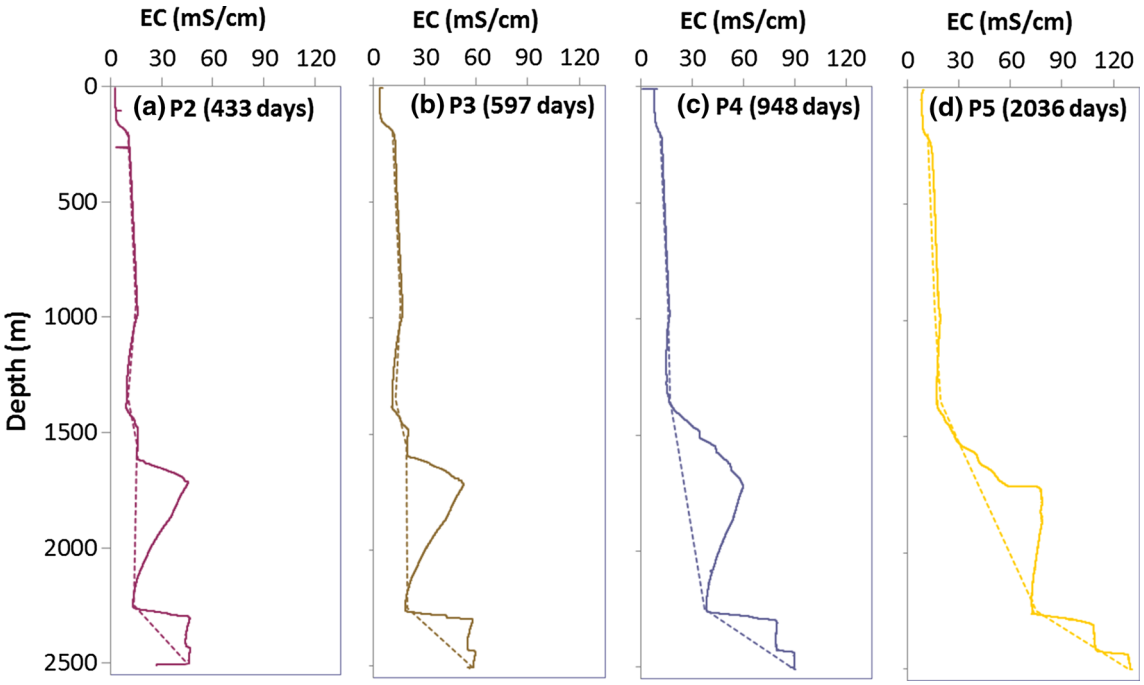

Fig. 6 Profiles (P2–P5) with baseline (*dotted line*) of individual profiles (*solid line*)

Now we need to evaluate β_1 and β_2, each of which is a ratio of the background diffusion-caused salinity inflow into the borehole over the time interval. For this, we take an approximate approach by taking the EC profiles and excluding the peaks by connecting the lower points between the peaks linearly (Fig. 6). These approximate baseline profiles are then used to calculate the difference profiles shown in Fig. 7, from which β_1 and β_2 are calculated. Since β_1 and β_2 are ratios of differences, the approximations used in their evaluations may be acceptable, as evidenced by the results.

Using the approximate procedure described above, the maximum formation water $EC_{R,max}$ at the bottom of the well was determined to be 124 and 152 mS/cm using the calculated values of β_1 and β_2, respectively, based on the two alternative combinations of long-term logging data. Although this procedure does not give us the same value for the maximum formation water EC in the deep well, we have obtained a narrow range of its value. The similarity of the two $EC_{R,max}$ values gives us some degree of confidence in our method. The estimated formation water EC as a function of depth of the well is plotted against the original EC profiles obtained from the FFEC logs in Fig. 8. The estimated formation water EC follows the profile well until the first peak at 1715 m in both cases but the calculated maximum formation water EC using P45–P34 (β_1 case) underestimates the observed EC at the deeper part of the well near 2400 m depth. This contradicts the conceptual

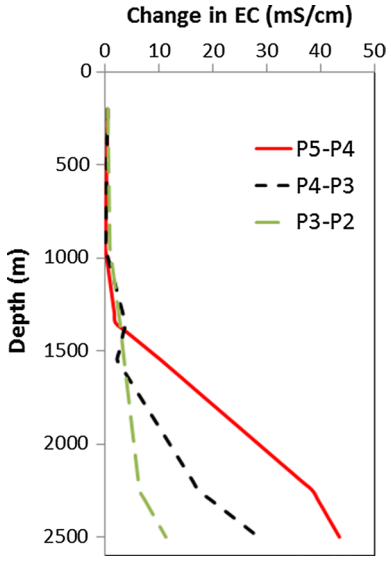

Fig. 7 Differences between the baseline profiles as shown in Fig. 6

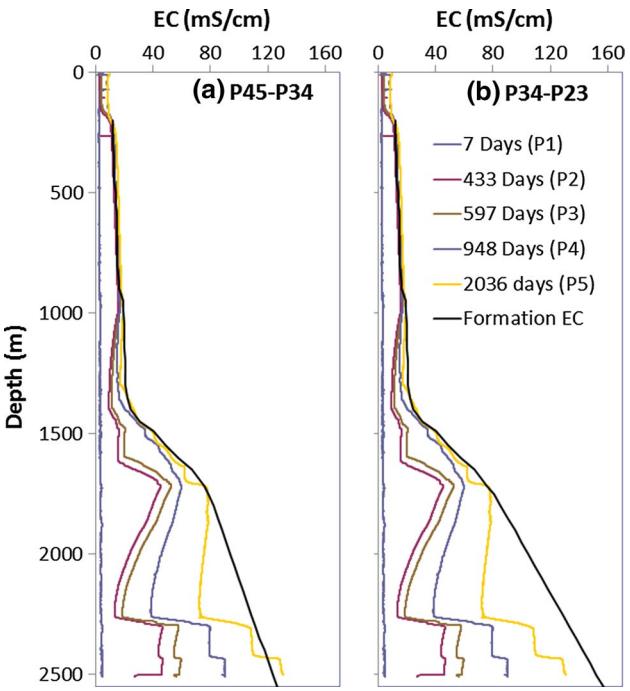

Fig. 8 Total and maximum fluid salinities in the formation calculated using the combination of **a** P45–P34 and **b** P23–P34. The profile of formation water EC in the *right figure* was adopted for subsequent calculations

model, and so the β_2 case with $EC_{R,max} = 152$ mS/cm will be used below.

Background EC profiles

In order to verify the calculated formation water EC along the wellbore using the mass balance approach, we used the rate of salinity (EC) diffusion obtained through profile P4–P3 in Fig. 4. The total mass of salt that entered into the borehole over the time period from T_3 to T_4 was obtained by integrating the background salt mass under the profile P4–P3. Then the constant term "α" can be calculated by rearranging Eq. (5) as follows:

$$\alpha = \frac{\Sigma M(P_4 - P_3)}{\left(\sum C_R - \sum C_{av}(P_{34})\right)T_{34}} \tag{9}$$

After knowing α, it is then possible to obtain the mass flux (J) using Eq. (3) at discretization interval of 50 m for each profile to use in BORE-II code simulation. The simulated background profile as a result of diffusion along the wellbore was obtained using BORE-II code in terms of EC which is equivalent to salinity through Eq. (2), with the help of input mass flux and known simulation time (Fig. 9). The figure shows that the diffusion mixing grows with time but it also overestimates at 2250 m depth the initial profiles (Fig. 9a–c). This might have happened because of an outflow location at that point, which was not considered in the diffusion mixing calculations.

The value of diffusion coefficient D controlling salinity flux from formation water to the wellbore can be evaluated from Eq. (3), based on the calculated mass flux J, ΔC, and by setting $H = 50$ m, and $R_{large}/r_w = 4$. The result for D thus obtained is 8×10^{-10} m^2/s. This is within an order of magnitude as the product of porosity (e.g., 10 %) times the diffusion coefficient of ions in water (~10^{-9} m^2/s, Dominoco and Schwartz 1998).

Results from long-term profiles

Peak EC profiles, flow pattern, and EC variation in the borehole

After estimating the background EC mass flux at 50-m intervals along the borehole and using the estimated formation water EC with $RC_{R,max}$ value of 152 mS/cm at 2500 m depth, as shown in Fig. 10a, the BORE-II code is then used to simulate all four profiles in Fig. 11, using a trial and error fitting method in order to determine flow rates at inflow and outflow zones intercepted by the borehole. Figure 10b shows the inflow and outflow locations and the qualitative representation of flow direction along the wellbore (also indicated in Kukkonen et al. 2011). The simulated profiles match well for all depth locations in the wellbore at each point of measured data in Outokumpu well (Fig. 11). Based on the measured EC profiles at Outokumpu well and the simulation from FFEC method, we were thus able to determine our best-fit EC depth profile of formation water in the surrounding rocks of the deep well (with $EC_{R,max} = 152$ mS/cm), as well as inflows

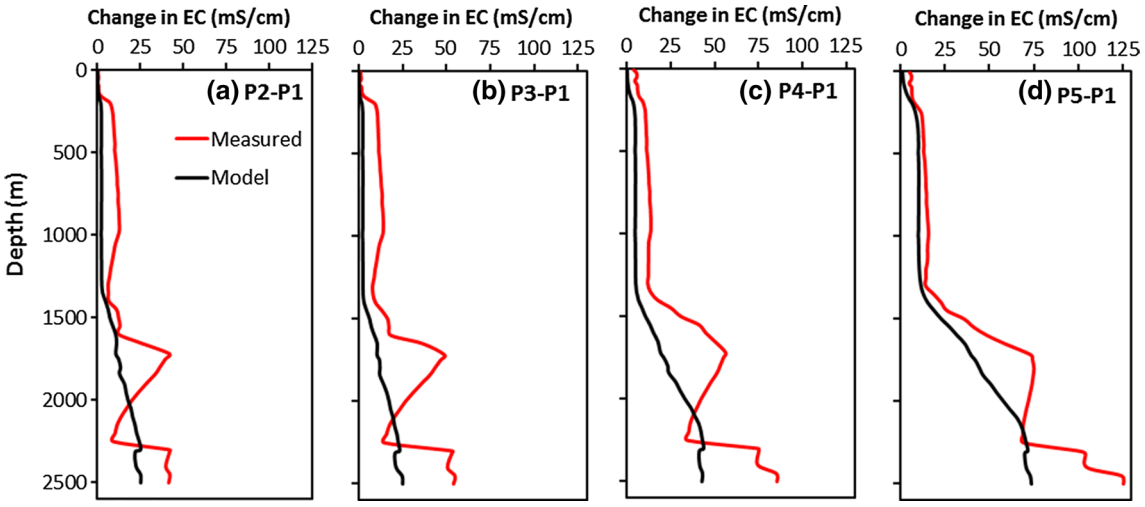

Fig. 9 Difference between measured profile and initial profile (*red lines*) and background profile calculated with BORE-II using inflow points at 50-m intervals to represent diffusive flux (*black lines*)

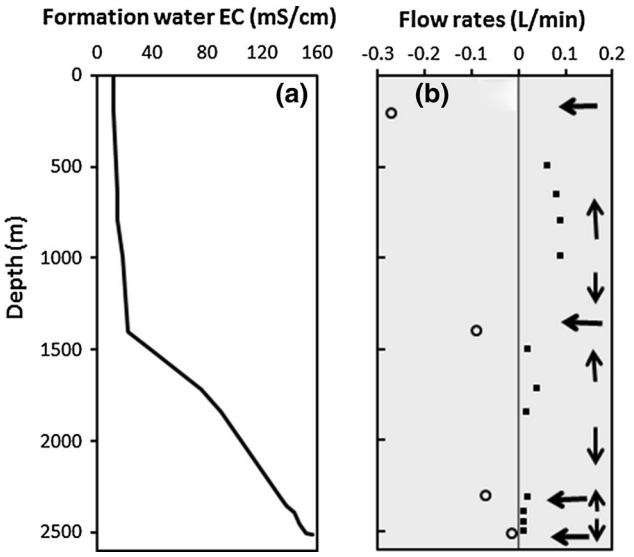

Fig. 10 **a** Variation of EC with depth used for BORE-II simulation, **b** location of inflow and outflow point and the direction of water flow (using *arrow line*)

and outflows at 15 depth levels along the deep well. The results are shown in Table 2. The flow rates are relatively high (60–90 mL/min) at the top part of the well (<1400 m) as compared to the lower part of the well (10–18 mL/min for >1400 m, except 38 mL/min at the 1715 m depth). As a result, the top part of the well got saturated in EC value relatively early. The estimated formation water EC was relatively small and less variable (12–22 mS/cm) until 1400 m depth but increased sharply from 1400 m until the deeper part of the well and reached to an estimated maximum EC_R of 152 mS/cm at 2500 m depth.

Hydraulic conductivity of fracture zones in the borehole

Table 2 (in column 2) gives the inflow rates as a function of depth. In order to evaluate the hydraulic conductivity of all the deeper conductive zones intercepted by the borehole using FFEC method, we need to start with a known value of hydraulic conductivity at one depth. The hydraulic conductivity of the conductive fracture zone at 990 m depth (957–997 m interval) has been estimated based on a drill stem test during a drilling break after drilling reached a depth of 997 m (Ahonen et al. 2011; Kietäväinen et al. 2013). In that test, the water from the isolated section was allowed to flow into the pipe and the change in pressure was monitored at the same time. The hydraulic conductivity was then estimated on the basis of water rise in the pipe analogous to a slug test over the 40-m interval assuming the bottom boundary to be impermeable (Ahonen et al. 2011). The hydraulic conductivity at 957- to 997-m interval was evaluated to be 0.032 mm/min. A similar test was done also at a higher interval, 480–550 m, whose hydraulic conductivity was found to be 0.45 mm/min.

Since we have the inflow rates q obtained in this study based on FFEC method (Table 2, column 2), it is possible to estimate the hydraulic conductivity K of each of the fracture zones using the one independently estimated value at 990 m based on the Darcy's law:

$$q = 2\pi r_w H \cdot K \cdot \frac{\partial h}{\partial r} \tag{10}$$

where q is the flow rate, K is the hydraulic conductivity, and $\partial h/\partial r$ is the pressure gradient. Under the assumption of constant $\partial h/\partial r$ for all the inflow zones, then q is

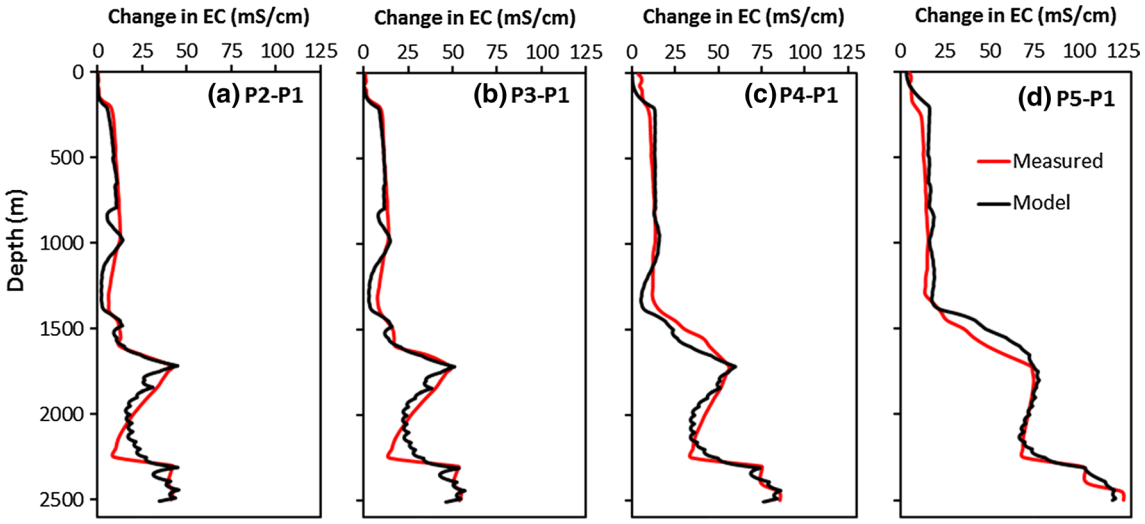

Fig. 11 Modeling/matching of FFEC logging data collected at different time intervals for: **a** P2–P1, 426 days, **b** P3–P1, 590 days, **c** P4–P3, 941 days, and **d** P5–P1, 2029 days

Table 2 Inflow and outflow rates with their corresponding formation water EC at different depths where the borehole intersects hydraulically conducting fractures

Depth (m)	Flow rate (mL/min)	Formation water EC (mS/cm)	Hydraulic conductivity (mm/min)
200	−270	–	–
490	60	14	0.021[b]
650	80	15	0.028[b]
790	90	15	0.032[b]
990 (957–997)[a]	90	19	0.032[a]
1400	−90	–	–
1500	18	40	0.006
1715	38	76	0.013
1840	16	90	0.006
2300	−70	–	–
2310	20	138	0.007
2390	10	143	0.004
2450	11	147	0.004
2500	11	152	0.004
2510	−14	–	–

[a] Independent data from drill stem test (Ahonen et al. 2011) used to calculate the results of hydraulic conductivity in column 4

[b] With uncertainty of more than a factor of 10 (see "Discussion" section)

proportional to K. Thus, the inflow rates from Table 2 (column 3) can be used to estimate their hydraulic conductivities (Table 2, column 4) by a simple ratio with the 990-m data. The assumption of constant $\partial h/\partial r$ value for all inflow zones is probably not true. If there is a difference of a factor of 2 between its value at a particular inflow zone and the average value over all inflow zones, then this would imply that the estimated hydraulic conductivity values (Table 2, column 4) have an inaccuracy of a factor of 2. It is noted that the hydraulic conductivity at the 490 m depth calculated from this ratio method turns out to be equal to 0.021 mm/min, which is an order of magnitude lower than that measured independently by the drill stem test at the 480- to 550-m interval. However, the sensitivity analysis presented in the next section indicates that the EC data in the shallow part of the borehole are very insensitive to the hydraulic conductivities values of inflows at the upper part of the well (>1400 m). Changing the hydraulic conductivity value at the 480- to 550-m interval to 0.45 mm/min would not change the EC profile at that part of the borehole. In other words, FFEC logging data should not be used to evaluate inflow rate and hydraulic conductivity value of inflow

zones situated in the shallower part of logging data where EC has been saturated (i.e., reached a stable value).

Discussion

This study is based on the analysis of EC data from a single deep borehole at Outokumpu, Finland. We are able to estimate the flow rate variability along the deep borehole and EC of formation water as a function of depth. Temperature logging data are also available from the deep borehole and in principle these can also be used to estimate flow rate from the well. However, thermal heat transfer is a much stronger diffusive process than that of salinity (or equivalent EC), so that temperature profiles show very smeared out trend over the depth of the borehole and distinct peaks were not found at inflow points (Fig. 1; Kukkonen et al. 2011). Thus, while thermal data can yield general flow rates in the borehole, the EC profiles can provide inflows as a function of depth with a resolution of decimeter. The previously made estimates of maximum flow rates in and out of the borehole based on thermal arguments (Kukkonen et al. 2012) are of the same order of magnitude as the total flow rates obtained in the present study, thus providing an independent comparison of the results and support our results. In general, the Outokumpu results obtained in this paper indicate a downward decreasing hydraulic conductivity of the fractured crystalline rock medium, in-line with results obtained elsewhere (Ingebritsen and Manning 1999).

The FFEC method has been used to understand the EC or salinity variation with depth, flow pattern, and hydraulic structure of a deep borehole and it is demonstrated to work well even in the long-term EC data over about 6 years. However, the lack of EC data at early times with shorter intervals for the shallow high conductive zones (<1400 m in the current study) makes it impossible to determine their inflow rate values accurately even in the first step from P1 to P2 in this study, with data showing already a saturated EC value. Hence, the estimation of flow rates and their corresponding hydraulic conductivity values were very inaccurate for those top 1000 m. A sensitivity analysis was applied at the upper part of the wellbore (at 490 m from top) and at one of the conductive fractures at lower part of the well (1715 m), which is shown in Fig. 12. The results show that an increase in flow rate by 10 times at 490 m does not change the EC of the wellbore water at that depth because of complete saturation at these shallow conductive zones. However, a large impact in EC was noticed for changing the inflow at 1715 m depth by 1.5 times of its original value. In other words, the estimated hydraulic conductivity value for 490-m zone has an uncertainty of more than a factor of 10, but the hydraulic conductivity value determined at 1715 m has an uncertainty of less than

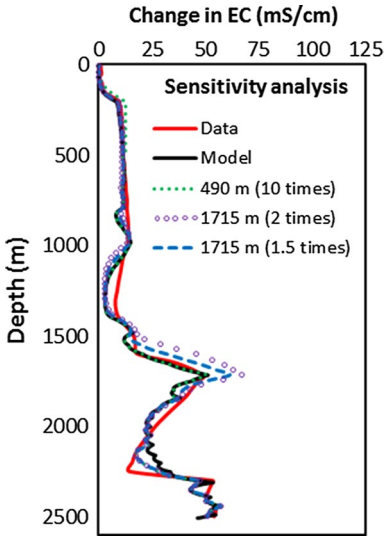

Fig. 12 Sensitivity analysis of model fitting on changes in inflow rates at two inflow depths, 490 and 1715 m, respectively. Results are shown for the flow rate at 490 m being increased by 10 times the best-fit value, and for the flow rate at 1715 m being increased by 1.5 and then by 2 times the best-fit value

a factor of 1.5. To determine the hydraulic conductivity of 490-m zone more accurately would require a few additional short-interval FFEC logging within the 1-year lapse between P1 and P2.

A pumping test at early time or FFEC logging at an early time in the well-testing mode for a few days can be done in order to estimate the flow rates of high conductive zones and for the whole well much more accurately. Furthermore, in the well-testing mode, the multi-rate FFEC logging method (Tsang and Doughty 2003) can be used to evaluate the difference in hydraulic heads among the inflow zones.

Concluding Remarks

This study shows that a long-term (up to 6 years) monitoring of fluid electrical conductivity in a deep borehole can be analyzed to yield meaningful results. In the case of the Outokumpu, it has been successfully analyzed using FFEC analysis technique to obtain the inflow/outflow points, their rates, and accounting for internal flow within the wellbore. It is possible to estimate EC of the surrounding formation water (EC_R as a function of depth) in the deep subsurface layers using only five logging profiles collected at irregular and long time intervals. Based on the available data and modeling results, a EC_R profiles with $EC_{R,max}$ equal to 152 mS/cm can be suggested for Outokumpu well (Fig. 10a). In addition, it is also possible to estimate the hydraulic conductivity structure and values all along

the depth of the well (Table 1, column 4). Note that the Outokumpu EC data were not obtained with the specific purpose of conducting the analysis presented in this paper. Based on this study, we suggest that FFEC logging should be included in the planning of a deep borehole. For a deep well, firstly FFEC logging in a well-test mode (see "FFEC logging method" section) should be conducted when the well drilling is completed, and then FFEC logging in a monitoring mode should be implemented with early time intervals in months followed by later time interval in years. Overall, the present study suggests and demonstrates the potential of long-term EC monitoring in a deep borehole and the use of the FFEC analysis method to obtain a detailed EC depth profile and hydraulic information such as the depths of hydraulically conductive fracture zones and their conductivity values.

Acknowledgments The authors cordially acknowledge the Swedish Geological Survey (SGU), Grant Number 1724, for providing financial support to the research reported in this paper. We are most grateful to the NEDRA and ICDP-OSG logging teams, especially Jochem Kueck, Christian Carnein, and Karl Bohn for collecting the logging data. We also acknowledge ICDP for supporting the post-drilling logs.

References

Ahonen L, Kietäväinen R, Kortelainen N, Kukkonen IT, Pullinen A, Toppi T, Bomberg M, Itävaara M, Nousiainen A, Nyyssönen M, Öster M (2011) Hydrological characteristics of the Outokumpu deep drill hole, in Outokumpu Deep Drilling Project. In: Kukkonen IT (ed) Finnish Geological Survey (GTK) Special Paper 51, pp 151–168

Dominoco PA, Schwartz FW (1998) Physical and chemical hydrogeology. Wiley, New York

Doughty C, Tsang CF (2005) Signatures in flowing fluid electric conductivity logs. J Hydrol 310:157–180

Doughty C, Takeuchi S, Amano K, Shimo M, Tsang CF (2005) Application of multi-rate flowing fluid electric conductivity logging method to well DH-2, Tono Site, Japan. Water Resour Res 41:W10401. doi:10.1029/2004WR003708

Doughty C, Tsang CF, Yabuuchi S, Kunimaru T (2013) Flowing fluid electric conductivity logging for a deep artesian well in fractured rock with regional flow. J Hydrol 482:1–13

Follin S, Hartley L, Rhén I, Jackson P, Joyce S, Roberts D, Swift B (2014) A Methodology to Constrain the parameters of a hydrogeological discrete fracture network model for sparsely fractured crystalline rock, exemplified by data from the proposed high-level nuclear waste repository site at Forsmark, Sweden. Hydrogeol J 22:313–331

Frampton A, Cvetkovic V (2010) Inference of field-scale fracture transmissivities in crystalline rock using flow log measurements. Water Resour Res 46:W11502. doi:10.1029/2009WR008367

Ingebritsen SE, Manning CE (1999) Geological implications of a permeability-depth curve for the continental crust. Geology 27:1107–1110

Itävaara M, Nyyssönen M, Kapanen A, Nousiainen A, Ahonen L, Kukkonen I (2011a) Characterization of bacterial diversity to a depth of 1500 m in the Outokumpu deep borehole, Fennoscandian Shield. FEMS Microbiol Ecol 77:295–309

Itävaara M, Nyyssönen M, Bomberg M, Kapanen A, Nousiainen A, Ahonen L, Hultman J, Paulin L, Auvinen P, Kukkonen IT (2011b) Microbiological sampling and analysis of the Outokumpu Deep Drill Hole biosphere in 2007–2009. Geol Survey Finl Special Paper 51:199–206

Kern H, Mengel K, Strauss KW, Ivankina TI, Nikitin AN, Kukkonen IT (2009) Elastic wave velocities, chemistry and modal mineralogy of crustal rocks sampled by the Outokumpu scientific drill hole: evidence from lab measurements and modeling. Phys Earth Planet Inter 175:151–166

Keys WS (1986) Analysis of geophysical logs of water wells with a microcomputer. Ground Water 24:750–760

Kietäväinen R, Ahonen L, Kukkonen IT, Hendriksson N, Nyyssönen M, Itävaara M (2013) Characterisation and isotopic evolution of saline waters of the Outokumpu deep drill hole, Finland—implications for water origin and deep terrestrial biosphere. Appl Geochem 32:37–51

Kietäväinen R, Ahonen L, Kukkonen IT, Niedermann S, Wiersberg T (2014) Noble gas residence times of saline waters within crystalline bedrock, Outokumpu deep drill hole, Finland. Geochim Cosmochim Acta 145:159–174

Kukkonen IT (2011) (ed) Outokumpu Deep Drilling Project 2003–2010: Geological Survey of Finland, Special Paper 51, 252 p

Kukkonen IT, Rath V, Kivekäs L, Safanda J, Cermak V (2011) Geothermal studies of the Outokumpu deep drill hole, Finland: vertical variation in heat flow and palaeoclimatic implications. Phys Earth Planet Inter 188:9–25

Kukkonen IT, Heinonen S, Heikkinen P, Sorjonen WP (2012) Delineating ophiolite-derived host rocks of massive sulfide Cu–Co–Zn deposits with 2D high-resolution seismic reflection data in Outokumpu, Finland. Geophysics 77:WC213–WC222

Ludvigson JE, Hansson K, Rouhiainen P (2002) Methodology study of Posiva difference flow Meter in borehole KLX02 at Laxemar. Report, Swedish Nuclear Fuel and Waste Management Co (SKB), Stockholm, Sweden

Mendoza A, Torres-Verdin C, Preeg B (2010) Linear iterative refinement method for the rapid simulation of borehole nuclear measurements: part I—vertical wells. Geophysics 75:E9–E29

Molz FJ, Morin RH, Hess AE, Melville JG, Guven O (1989) The impeller meter for measuring aquifer permeability variations: evaluation and comparisons with other tests. Water Resour Res 25:1677–1683

Nurmi PA, Kukkonen IT (1986) A new technique for sampling water and gas from deep drill holes. Can J Earth Sci 23:1450–1454

Nyyssönen M, Hultman J, Ahonen L, Kukkonen I, Paulin L, Laine P, Itävaara M, Auvinen P (2013) Taxonomically and functionally diverse microbial communities in deep crystalline rocks of the Fennoscandian shield. ISME J. doi:10.1038/ismej.2013.125

Öhberg A, Rouhiainen P (2000) Posiva groundwater flow measuring techniques. Working Report. Posiva Oy, Eurajoki

Paillet FL (1991) Use of geophysical well logs in evaluating crystalline rocks for siting of radioactive waste repositories. Log Anal 32:85–107

Paillet FL (1998) Flow modeling and permeability estimation using borehole flow logs in heterogeneous fractured formations. Water Resour Res 34:997–1010

Schijns H, Schmitt DR, Heikkinen PJ, Kukkonen IT (2012) Seismic anisotropy in the crystalline upper crust: observations and modelling from the Outokumpu scientific borehole, Finland. Geophys J Int 189:541–553

Sharma P, Tsang CF, Doughty C, Niemi A, Bensabat J (2015) Feasibility of long-term passive monitoring of deep hydrogeology with flowing fluid electric conductivity logging method. In: Faybishenko B, Gale J, Benson S (ed) Fluid dynamics in complex fractured-porous systems, geophysical monograph, vol 210. John Wiley & Sons, Inc. ISBN: 978-1-118-87720-3

Snoeyink VL, Jenkins D (1980) Water chemistry. Wiley, New York

Tsang CF, Doughty C (2003) Multirate flowing fluid electric conductivity logging method. Water Resour Res 39(12):1354–1362. doi:10.1029/2003WR002308

Tsang CF, Hufschmied P, Hale FV (1990) Determination of fracture inflow parameters with a borehole fluid conductivity logging method. Water Resour Res 26:561–578

Walton WC (1970) Groundwater resource evaluation. McGraw-Hill, New York

Zemanek J, Glenn EE, Norton LJ, Caldwell RL (1970) Formation evaluation by inspection with the borehole televiewer. Geophysics 35:254–269